Biosensors and Bioelectronics 26 (2011) 3420–3426

Contents lists available at ScienceDirect

Biosensors and Bioelectronics

journal homepage: www.elsevier.com/locate/bios

Construction and application of an amperometric xanthine biosensor based on zinc oxide nanoparticles–polypyrrole composite film

Rooma Devi [a], Manish Thakur [b], C.S. Pundir [a,*]

[a] Department of Biochemistry, M.D. University, Rohtak-124 001 (Haryana), India
[b] Department of Pathology, Dr Sur Homeopathic College and Hospital, New Delhi, India

ARTICLE INFO

Article history:
Received 8 December 2010
Accepted 11 January 2011
Available online 19 January 2011

Keywords:
Xanthine
Xanthine oxidase
Xanthine biosensor
Zinc oxide nanoparticles–polypyrrole film
Fish

ABSTRACT

Zinc oxide nanoparticles (ZnO-NPs) were synthesized from zinc nitrate by simple and efficient method in aqueous media at 55 °C without any requirement of calcinations step. A mixture of ZnO-NPs and pyrrole was eletropolymerized on Pt electrode to form a ZnO-NPs–polypyrrole (PPy) composite film. Xanthine oxidase (XOD) was immobilized onto this nanocomposite film through physiosorption. The ZnO-NPs/polypyrrole/Pt electrode was characterized by Fourier transform infrared (FTIR), cyclic voltammetry (CV), X-ray diffraction (XRD), scanning electron microscopy (SEM), transmission electron microscopy (TEM) and electrochemical impedance spectroscopy (EIS) before and after immobilization of XOD. The XOD/ZnO-NPs–PPy/Pt electrode as working electrode, Ag/AgCl as reference electrode and Pt wire as auxiliary electrode were connected through a potentiostat to construct a xanthine biosensor. The biosensor exhibited optimum response within 5 s at pH 7.0, 35 °C and linearity from 0.8 μM to 40 μM for xanthine with a detection limit 0.8 μM (S/E = 3). Michaelis Menten constant (K_m) for xanthine oxidase was 13.51 μM and I_{max} 0.071 μA. The biosensor measured xanthine in fish meat and lost 40% of its initial activity after its 200 uses over 100 days, when stored at 4 °C.

1. Introduction

Xanthine (3,7-dihydro-purine-2,6-dione) present in most body tissues and fluids, is generated from guanine by guanine deaminase and from hypoxanthine by xanthine oxidase. Determination of xanthine level in blood and tissue is essential for diagnosis and medical management of various diseases like hyperuricemia, gout, xanthinuria and renal failure. A number of mild xanthine derived stimulants like caffeine and theobromine are present in tea and coffee. Fresh fish meat is required in food industries for manufacturing of high quality products. After the death of a fish, ATP is degraded into xanthine, which increases with storage. Thus xanthine attracts much attention as an indicator for fish freshness (Shan et al., 2009). Various methods have been devised for determination of xanthine like enzymic colorimetric (Berti et al., 1988), enzymatic fluorimetric, fluorometric mass spectrometry fragmentography (Olojoa et al., 2005), HPLC (Kock et al., 1993) and capillary column gas chromatography (Renata et al., 2002). However, these methods are cumbersome, time consuming and requires sample preparation. As compared to them, amperometric determination of xanthine by biosensors is comparatively more simple, rapid, sensitive and requires no sample preparation (Shah, 1996). In these biosensors, xanthine oxidase has been immobilized onto various supports such as polypyrrole film (Arslan et al., 2006), nafion membrane (Nakatani et al., 2005), self-assembled phospholipids membrane (Rehak et al., 1994), theophylline coated nylon mesh (Mao et al., 1999; Moody et al., 1987), cellulose acetate membrane (Basu et al., 2005), silk membrane (Mao et al., 2001) PVC membrane (Pundir et al., 2011) and silk fibroin membrane (Mulchandani et al., 1989). However these supports (film/membranes) had few drawbacks such as poor stability, reusability and slow electron transfer, while some membranes were fragile, non-conducting, non-elastic and had poor absorption ability. Recent xanthine biosensors were based on electrochemical hybrid electrodes using Cu(II) hypoxanthine absorptive complex at a hanging mercury drop electrode (HMDE) (Pei and Li, 2000), $CuPtCl_6$/GC (Hu et al., 2000), sodium montmrillonite-methyl violate carbon paste (Mao et al., 2001), carbon fiber microelectrodes (CFMEs) using nafion (Lui et al., 2004) and Au–colloid polypyrrole layer (Lui et al., 2004). These biosensors were also suffered from limited electron communication, complexity of immobilization and stability of enzymes. Ever since the conducting polymers were introduced by Diaz et al. (1979) by depositing thin films of polypyrrole (PPy) on an electrode using electro-oxidation, conducting polymers have attracted the attention of several workers. Currently, an intensive attention is being paid to the design of nano-devices, due to the growing miniatur-

* Corresponding author. Tel.: +91 9416492413.
E-mail addresses: pundircs@rediffmail.com, pundircs@gmail.com (C.S. Pundir).

0956-5663/$ – see front matter © 2011 Elsevier B.V. All rights reserved.
doi:10.1016/j.bios.2011.01.014

ization of microelectronic devices. Certain conducting polymer and nanoparticles (NPs) composites have already been reported in the literature, such as polyaniline/metaloxide NP composites (Nabid et al., 2008; Moghaddam and Nazari, 2008; Phang et al., 2008), PPy/TiO_2 (Liu et al., 2004), PPy/Ti (Roux et al., 2003), PPy/Au (Chem et al., 2006), PPy/Ag (Liu et al., 2006), PPy/Pt (Bose and Rajeshwar, 1992), and PPy/Pd (Cioffi et al., 2000). Nanostructure metal oxides are know to have unique ability to promote faster electron transfer kinetics between electrode and the active site of the desired enzyme (Pandey et al., 2008; Zhou et al., 2005; Kumar and Chen, 2008; Singh et al., 2007; Wang et al., 2006a). Among the metal oxide nanoparticles, ZnO-NPs have been exploited as a potential material for biosensing because of their unusual properties i.e., high surface area for strong adsorption (high isoelectric point 9.5), good biocompatibility, chemical stability, non toxicity and high electron communication. Nanoporous ZnO greatly enhances the surface area for strong adsorption of biomolecules (Singh et al., 2007; Wang et al., 2006b). These nonporous ZnO-NPs/ZnO nanorods/nanocombs have been employed for the fabrication of different biosensors such as glucose (Wang et al., 2006a), myoglobin (Zhao et al., 2006), microperoxidase, hydrogen peroxide (Zhu et al., 2007), phenol (Li et al., 2006), uric acid (Zhang et al., 2004), human IgG (Wang et al., 2006b) and cholesterol (Khan et al., 2008). To the best of our knowledge, no attempts have been made towards the development of a xanthine biosensor based on zinc oxide nanoparticles–polypyrrole composite (ZnO-NPs–PPy). We report here in the construction of a amperometric novel xanthine biosensor by immobilizating commercial XOD on ZnO-NPs–PPy composite film electrodeposited onto Pt electrode and its application.

2. Materials and methods

2.1. Materials

Xanthine oxidase (XOD) (E.C.1.1.3.2) from buttermilk (0.15 U/mg), xanthine from SRL, Mumbai and Pyrrole from Fluka, Mumbai were used. Pyrrole was stored below 5 °C in dark. All other chemicals were of AR grade.

2.2. Assay of xanthine oxidase

The assay of xanthine was carried out in a test tube as described by Westerfield et al. (1959) with modification and based on oxidation of xanthine to uric acid by xanthine oxidase. Assay mixture contained 1.8 ml of 50 mM sodium phosphate buffer (pH 7.0), 0.1 ml xanthine (0.15 mM) and 0.1 ml xanthine oxidase (0.15 U/mg). Increase in absorbance at 290 nm was read against blank in a UV spectrophotometer (Schimadzu, 1700). The activity was calculated as follows:

$$\text{Units/ml} = \frac{\Delta A/\text{min} \times 1000 \times 3\,\text{ml} \times \text{dilution}}{1.22 \times 10^4 \times 0.1\,\text{ml}}$$

$$\text{Extinction Coeff. of uric acid} = 1.22 \times 10^4\,\text{cm}^{-1}$$

2.3. Instruments

Autolab potentiostat/galvanostat (Eco Chemie, Netherlands) was used for amperometric measurements as well as electrochemical impedance spectroscopic measurements (0.01–105 Hz). A three electrode cell with XOD/ZnO-NPs–PPy/Pt electrode as the working electrode, Ag/AgCl electrode with saturated KCl as a reference electrode and platinum (Pt) wire as the counter electrode were used. UV–visible spectra from in UV–visible spectrophotometer (Make: Shimadzu, Model 160 A) and the FTIR spectra from FTIR spectrophotometer (Thermo Scientific, USA) were recorded. The morphological studies were carried out with scanning electron microscope (SEM) (Model Joel JSM-6510, Japan) at Department of Chemistry, M.D. University, Rohtak, powder X-ray diffraction (XRD) experiments were conducted on a X-ray diffractometer (Make: Rigaku, D/Max2550, Tokyo, Japan) at Department of Physics, G.J. University, Hisar, collecting data in steps of 2-theta from 20 to 70 (2-theta). The database of the Joint Committee on Powder Diffraction Standards (JCPDS) was used for phase identification.

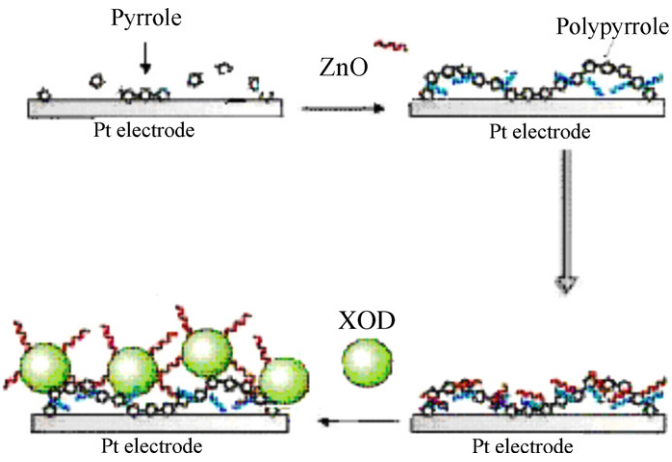

Scheme 1. Schematic representation of chemical reactions involved in fabrication of XOD/ZnO-NPs–PPy/Pt.

2.4. Construction of XOD/ZnO-NPs–PPy/Pt electrode

2.4.1. Preparation of ZnO-NPs

ZnO-NPs were prepared as described (Moghaddam et al., 2009) using a 0.45 M aqueous solution of zinc nitrate ($Zn(NO_3)_2{\cdot}4H_2O$) and 0.9 M aqueous solution of sodium hydroxide (NaOH). NaOH (100 ml) solution was heated at 55 °C. Zinc nitrate solution (50 ml) solution was added drop wise (slowly for 40 min) to the heated NaOH solution under high speed stirring. The beaker was sealed during this process for 2 h. The precipitated ZnO-NPs were cleaned with deionized water and ethanol, dried in air at 60 °C.

2.4.2. Electropolymerization of PPy on Pt electrode with ZnO-NPs

The surface of the Pt electrode (1.85 cm × 1 mm) was manually polished successively by 0.05 μM of alumina slurry on a polishing cloth, followed by a thorough distilled water rinsing. The electrode was then successively sonicated in ethanol and distilled water to remove the adsorbed particles. To electropolymerized pyrrole, 50 mg ZnO-NPs were added in 100 mM $NaClO_4$ (10 ml) and 30 mM pyrrole (4 ml). The polymerization of pyrrole was carried out by applying potentials to Pt working electrode at 100 mV/s. For control, a pure pyrrole was also polymerized under the similar conditions as mentioned above, but no ZnO-NPs were added in the polymerization electrolyte. The electropolymerization of pyrrole was studied by SEM.

2.4.3. Immobilization of XOD onto ZnO-NPs/PPy/Pt electrode

The proposed mechanism for preparation of ZnO-NPs/PPy/Pt electrode and immobilization of XOD onto this electrode is shown in Scheme 1. ZnO-NPs/PPy/Pt electrode was dipped into 10 μl solution of freshly prepared XOD containing 0.1 U and kept undisturbed for about 12 h at 4 °C. Finally, the electrode was immersed into 0.05 M sodium phosphate buffer (PBS) (pH 7.0) to wash out any unbound XOD from the electrode, surface. To measure activity of enzyme electrode a solution of 0.15 mM xanthine (0.1 ml) was added to 3 ml PBS (pH 7.0). The XOD/ZnO-NPs/PPy/Pt electrode

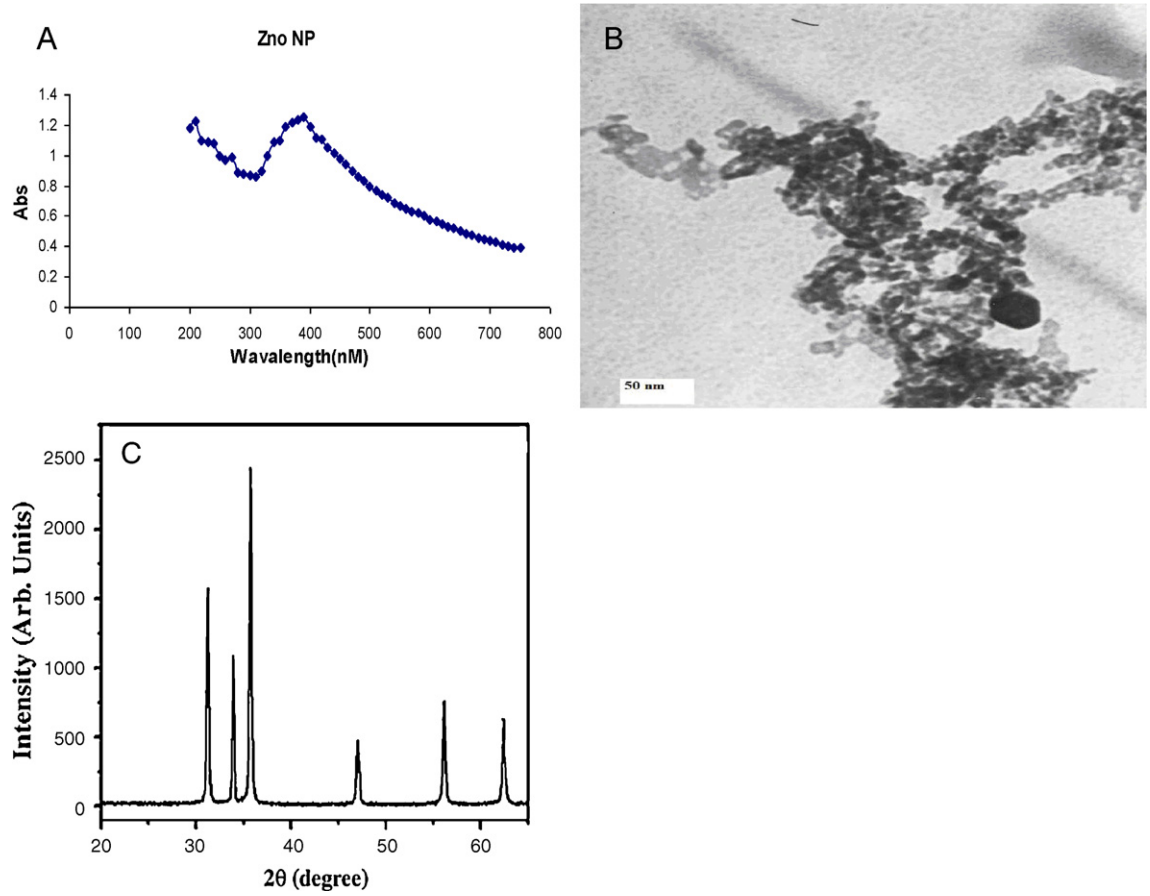

Fig. 1. (A) UV spectrum of ZnO-NPs, (B) transmission electron microscopic (TEM) images, of ZnO-NPs and (C) X-ray diffraction (XRD) pattern of taken from ZnO-NPs.

was immersed into this solution and incubated for 5 min at 25 °C. The electrode was taken out and the absorbance of the solution was noticed at 290 nm in a double beam UV spectrophotometer to measure the concentration of product. The fabricated electrode was characterized by SEM, Fourier transforms infrared (FTIR) spectroscopy and electrochemical impedance spectra (EIS). Enzyme electrode was stored at 4 °C when not in use.

2.5. Cyclic voltammetric measurement and testing of xanthine biosensor

Cyclic voltammogram (CV) of XOD/ZnO-NPs/PPy/Pt electrode was recorded in potentiostat–galvanostat from −0.2 to 0.8 V vs. Ag/AgCl as reference and Pt wire as counter electrode in a 15 ml (0.05 M) sodium phosphate buffer (pH 7.0) containing 0.15 mM xanthine (0.5 ml). The maximum response was observed at 0.38 V and hence subsequent amperometric studies were carried out at this voltage. For further amperometric studies, three electrodes were connected to a potentiostat/galvanostat and then immersed into 25 ml 0.05 M sodium phosphate buffer (pH 7.0) in a 50 ml beaker. The reaction was started by adding xanthine solution of different concentration in reaction mixture and the current (A) generated was recorded at 0.38 V.

2.6. Optimization of xanthine biosensor

The experimental conditions affecting the biosensor response were studied in terms of effect of pH, incubation temperature, time and substrate (xanthine) concentration. To determine optimum pH, the pH was varied from 3.0 to 8.0 at an interval of 0.5. Similarly optimum temperature was studied by incubating the reaction mixture at different temperature (20–50 °C) and time (1–40 s). The effect of xanthine concentration on biosensor response was determined by varying the concentration of xanthine from 0.8 μM to 200 μM.

2.7. Xanthine determination in fish meat

Labeo fish was purchased from a local market. Fish was chopped and homogenized in (5 ml 0.5 M $HClO_4$) until a fine paste was obtained for the precipitation of proteins in the sample. The denatured samples were mechanically stirred for 10 min and then centrifuged at 4000 rpm for 5 min. The supernatant was collected and its pH was adjusted to 7.0 with NaOH. The supernatant (fish meat extract) was diluted 10 times. Then these denatured sample solutions were divided into two parts. One part was used immediately and other was stored at room temperature. To determine xanthine content in fish sample, same procedure was used as described for sensor's response measurement under the optimal working conditions except that xanthine was replaced by the sample. The xanthine content was extrapolated from standard curve between xanthine concentrations vs. current (mA) prepared under optimal working conditions.

2.8. Evaluation

The performance of this biosensor was evaluated for linearity, analytical recovery and detection limit.

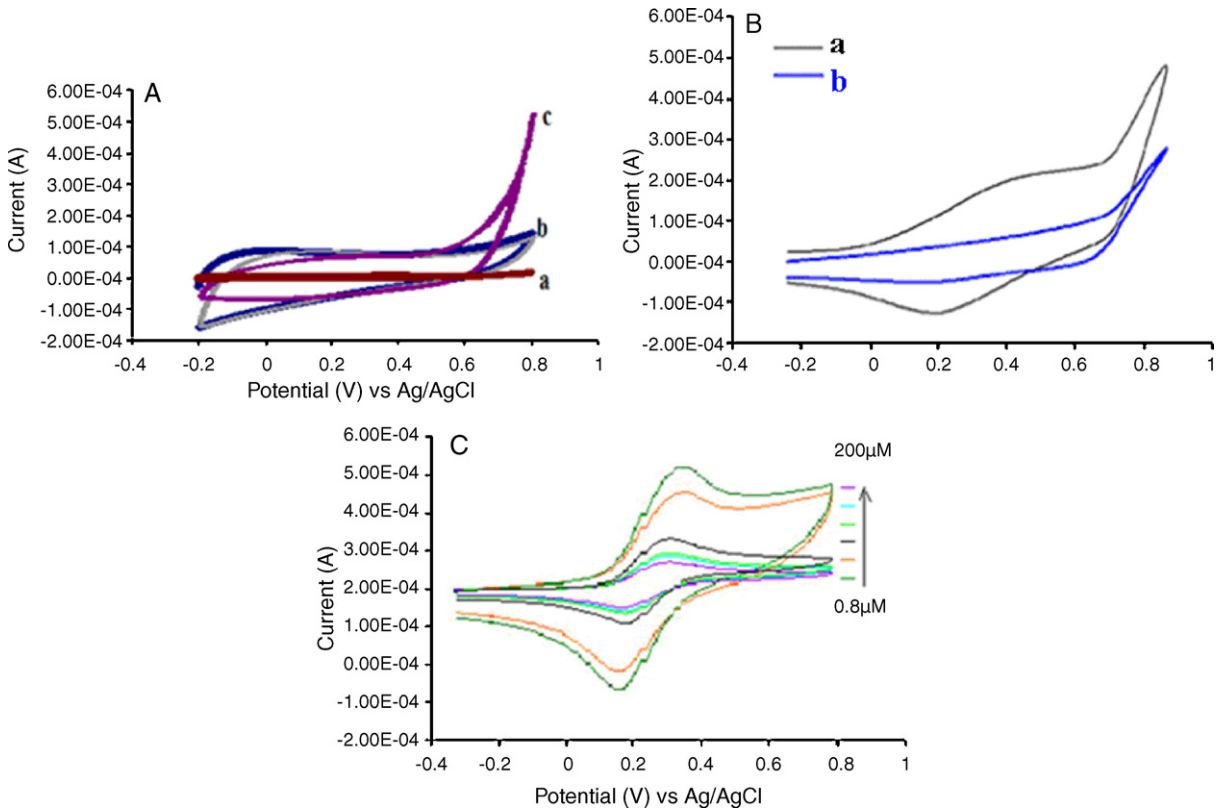

Fig. 2. Cyclic voltammogram for electrochemical deposition of (A) (a) Pt electrode, (b) PPy/Pt electrode, (c) ZnO-NPs–PPy/Pt electrode in 30 mM $NaClO_4$, (B) XOD/ZnO-NPs–PPy/Pt electrode a with xanthine b without xanthine phosphate buffer 50 mM, pH 7.0, 0.16 mM xanthine, (C) linear sweep voltammetry in phosphate buffer 50 mM, pH 7.0, xanthine (0.8–200 μM), (D) cyclic voltammetry of amperometric response studies of as a function of XOD/ZnO-NPs–PPy/Pt electrode in concentration from (0.8 to 200 μM) using phosphate buffer (50 mM, pH 7.0).

3. Results and discussion

3.1. Characterization of ZnO-NPs

The characterization of nanoparticles was carried out by UV spectrophotometric spectra (Fig. 1A) and transmission electron microscopy (TEM) images (Fig. 1B). The structure of ZnO-NPs was also characterized by XRD (Fig. 1C). All peaks were consistent with the peaks of ZnO nanoparticles with high crystallinity.

3.2. Construction of XOD/ZnO-NPs/PPy/Pt electrode

A method is described for construction of an electrochemical xanthine biosensor using xanthine oxidase (XOD) immobilized onto ZnO-NPs polypyrrole (PPy) composite film electrodeposited on the surface of a Pt wire through physiosorption to use it as working electrode along with Ag/AgCl as reference and Pt wire as auxillary electrode. The Scheme 1 summarizes reaction involved in fabrication of the xanthine biosensor based on immobilization of XOD onto ZnO-NPs/PPy/Pt electrode. The ZnO-NPs/PPy/Pt electrode potential peaks were not modified during cycling between −0.2 and +0.8 V. This explains that the structural properties of deposit film were electrochemically stable. The composite material had the same electrochemical behavior as observed for the PPy. Fig. 2A shows the cyclic voltammogram (CVs) recorded in a solution of 30 mM pyrrole in 100 mM $NaClO_4$, on a Pt substrate electrode and also with ZnO-NPs, dispersed in electrolyte solution to compares the influence of ZnO-NPs in the electropolymerization of pyrrole which indicates that the addition of ZnO NPs significantly increase the recorded currents at the same applied potentials. It can be concluded that electropolymerization of PPy/ZnO NPs composite layers is easier than the pure PPy layers because ZnO NPs exhibit interesting properties including high catalytic efficiency and strong adsorption ability (Kumar and Chen, 2008; Moghaddam et al., 2009).

In Fig. 2B XOD/ZnO-NPs/PPy/Pt electrode and its cyclic voltammogram has taken in presence of xanthine (a) and absence of xanthine (b). The oxidation peak seen at 0.38 V corresponding to the oxidation of H_2O_2 arisen due to the enzymatic reaction between xanthine oxidase and xanthine (Fig. 2B). The increase in the value of the oxidation current with increase in xanthine concentration resulted due to the increased concentration of H_2O_2 during enzymatic reaction. The cyclic voltammogram corresponding to the modified electrode is shown in Fig. 2C of amperometric response studies of as a function of XOD/ZnO-NPs–PPy/Pt electrode in concentration from (0.8–200 μM) using phosphate buffer (50 mM, pH 7.0). The electrochemical reactions involved in response measurement of xanthine biosensor are given below

$$\text{Xanthine} + O_2 + H_2O \xrightarrow{\text{XOD on hybrid film}} \text{Uric acid} + H_2O_2$$

$$H_2O_2 \xrightarrow{0.38\,V} 2H^+ + 2e^- + O_2$$

$$2e^- \xrightarrow{\text{ZnO-NPs–PPy}} \text{Pt electrode}$$

3.3. Surface characterization by SEM

The surface morphologies of PPy/Pt electrode, ZnO-NPs–PPy/Pt electrode and XOD/ZnO-NPs/PPy/Pt electrode were studied by SEM (Fig. 3). PPy/Pt electrode showed homogenous surface (Fig. 3a),

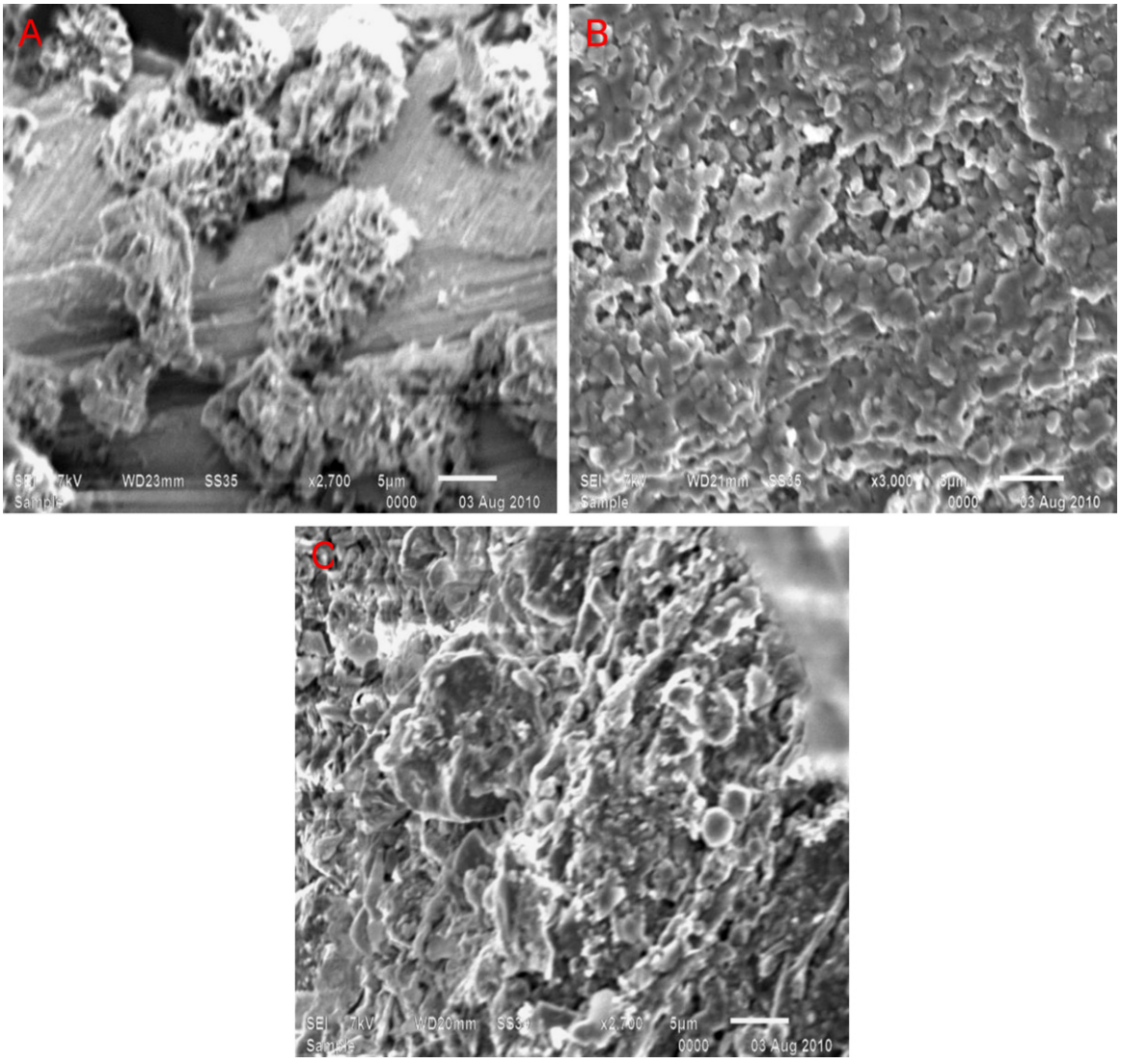

Fig. 3. SEM images of (A) PPy/Pt electrode, (B) ZnO-NPs–PPy/Pt electrode and (C) XOD/ZnO-NPs–PPy/Pt electrode.

whereas the ZnO-NPs/PPy/Pt electrode has uniform granular porous morphology attributed to the homogeneous dispersion of ZnO nanoparticles in PPy (Fig. 3b) network. On immobilization of XOD, the globular structural morphology of ZnO-NPs/PPy changes into the regular form due to the electrostatic interaction between ZnO-NPs/PPy with XOD (Fig. 3c).

3.4. FTIR spectra

Fig. 4(i) shows FTIR spectrum of pure KBr. Fig. 4(ii) shows FTIR spectrum of ZnO with a characteristic IR peak being observed at 412 cm^{-1}, FTIR spectrum of PPy/ZnO composite on Pt electrode, exhibits absorption peaks at 1547 and 1343.93 cm^{-1} for typical pyrrole ring vibration and that of =C–H in plane vibration peaks at 1294, 1045 cm^{-1}. Fig. 4(iii) shows a broad peak at 1164 cm^{-1} which is assigned as N–C stretching band and bands observed at 763, 500 cm^{-1} for the presence of polymerized pyrrole and that of metal oxide band at 444 cm^{-1} and 1625.88 cm^{-1} due to the addition of carbonyl and amino groups confirming the binding of xanthine oxidase with the ZnO-NPs/PPy matrix.

3.5. Electrochemical impedance measurements

Fig. 5 shows electrochemical impedance spectra (EIS) of (a) Pt electrode (b) ZnO-NPs–PPy/Pt electrode (c) PPy/Pt electrode and (d) XOD/ZnO-NPs/PPy/Pt electrode, respectively. The charge transfer process in XOD/ZnO-NPs/PPy/Pt electrode was studied by monitoring charge transfer resistance (RCT) at the electrode and electrolyte interface. The value of the electron transfer resistance (semicircle diameter) (RCT) depends on the dielectric and insulating features at the electrode/electrolyte interface. The RCT values for Pt electrode, ZnO-NPs/PPy/Pt, PPy/Pt, and XOD/ZnO-NPs/PPy/Pt electrodes were 0.8912, 1.412, 1.5320 and 9.645, respectively. The increased RCT value of XOD/ZnO-NPs/PPy/Pt electrode was due to the immobilization of XOD onto ZnO-NPs/PPy/Pt surface. The electron transfer via redox couple was hindered by the presence of xanthine oxidase on the electrode surface.

3.6. Optimization of experimental conditions

The experimental conditions affecting the biosensor response were studied in terms of effect of pH, incubation temperature, time and substrate (xanthine) concentration. The optimum current was

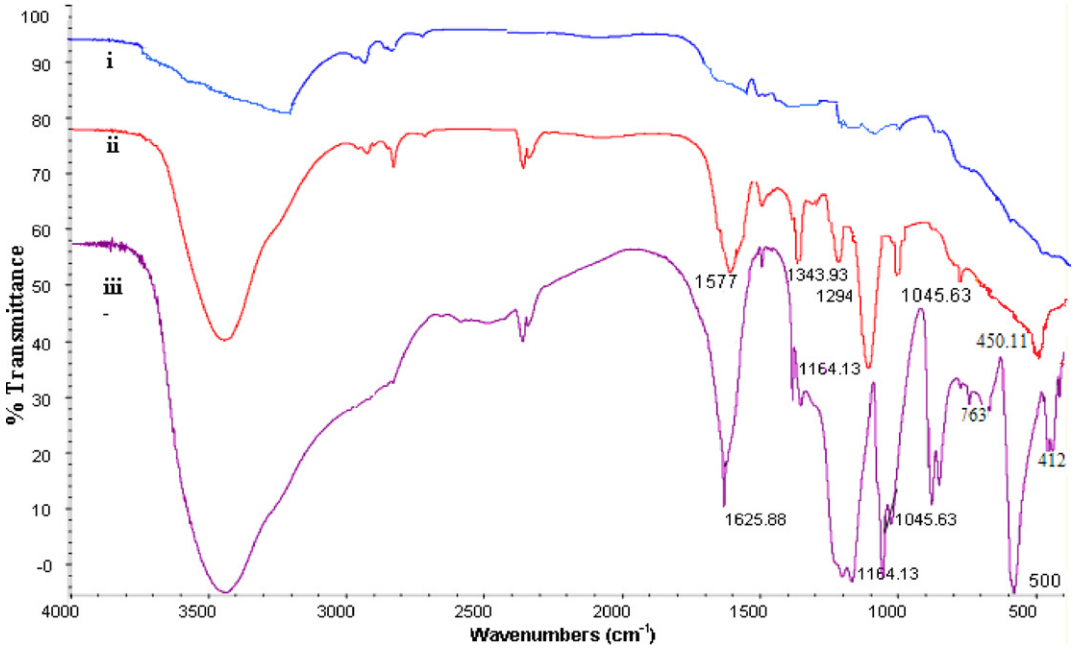

Fig. 4. FTIR spectra of (i) KBr, (ii) ZnO-NPs–PPy/Pt and (iii) XOD/ZnO-NPs–PPy/Pt electrode.

obtained within 4 s at pH 7 and 35 °C. There was a hyperbolic relationship between biosensor response and xanthine concentration from 0.8 μM to 200 μM, after 40 μM which it was constant. The Lineweaver–Burk plot between 1/*I* (mA) and 1/[xanthine] yielded a K_m 13.51 μM and I_{max} 0.071 μA indicating increased affinity of enzyme towards substrate (xanthine) after immobilization (K_m free xanthine oxidase 0.82×10^{-2} M), which might be due to enhanced diffusion of xanthine through composite film.

3.7. Evaluation of xanthine biosensor

The following parameters were studied to evaluate the performance of this biosensor.

3.7.1. Linearity

There was a linear relationship between xanthine concentration ranging from 0.8 to 40 μM and current (A), which is better than the earlier biosensor based on Nafion coated Pt electrode (2–18.5 μM) (Nakatani et al., 2005) but lower than that of carbon nanotube (CNT) modified carbon paste electrode (1–100 μM) (Anik and Cubukcu, 2008) and comparable to modified graphite electrode coated with gelatin (upto 40 μM) (Dimcheva et al., 2002)

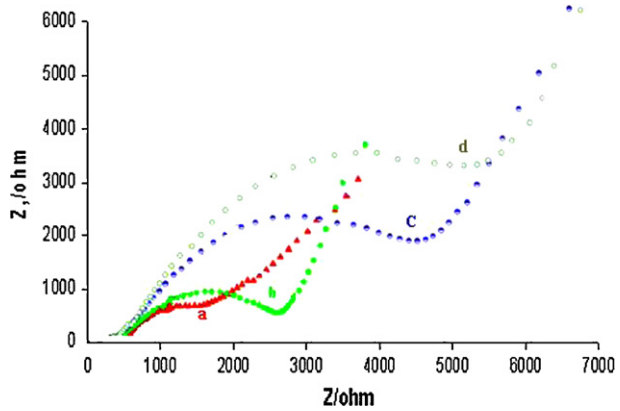

Fig. 5. Impedance spectra of (a) Pt electrode, (b) ZnO-NPs–PPy/Pt electrode, (c) PPy/Pt electrode and (d) XOD/ZnO-NPs–PPy/Pt electrode in phosphate buffer (50 mM, pH 7.0,100 mM $NaClO_4$) containing $[K_3Fe(CN)_6]$ (5 mM).

3.7.2. Detection limit

The detection limit of the biosensor was 0.8 μM (S/E = 3), which is lower than that of modified graphite electrode coated with gelatin (4.5 μM) (Dimcheva et al., 2002), polypyrrole modified film (400 μM) (Arslan et al., 2006) but higher than that of self-assembled biotinylated phospholipids membrane (0.02 μM) (Rehak et al., 1994) & $CuPtCl_6$/Glassy carbon (0.1 μM) (Hu et al., 2000) and comparable to FeTPP-NPs modified glassy carbon (1 μM) (Li et al., 2008) & modified carbon paste electrode (1 μM) (Anik and Cubukcu, 2008)

3.7.3. Xanthine in fish meat

The xanthine concentration in fish meat was determined by the present biosensor at different storage time ranging from 1 to 18 days at room temperature. Xanthine level was increased as the storage time was increased. It was double after 10th days than that on day 1 (Supplementary Fig. 1)

3.7.4. Analytical recovery

Analytical recoveries of exogenously added xanthine (10 mg/l, 20 mg/l) in fish sample by present method were 94.2% and 95.1%, respectively, showing the reliability of the method.

3.7.5. Precision study

In order to check the repeatability and reproducibility of the method, the xanthine content in same fish sample was determined five times on a single day (within batch) and again after storage at −20 °C for one week (between batch). The results showed that determinations were almost consistent and within and between batch coefficients of variation (CV) for fish sample determination were <5.1% and <5.34%, showing the good reproducibility and reliability of the method.

3.7.6. Accuracy

To know the accuracy of present method, values of xanthine in fish sample were determined by enzymic colorimetric

method (x) and by the present method (y). The xanthine values obtained by the present biosensor matched with enzymic colorimetric method with a good correlation ($r = 0.93$, significant at 1% level).

3.8. Long-term stability of electrode

To examine the long-term storage stabilities, the activity of XOD/ZnO-NPs/PPy/Pt electrode was tested with respect to storage time. After each experiment, the sensor was washed with buffer solution and stored at 4 °C. Studies revealed that the electrode lost only 40% of its initial activity its 200 regular uses over 100 days.

4. Conclusion

The use of a nanocomposite thin film of ZnO-NPs and PPy electrodeposited on the surface of Pt surface electrode as a support for immobilization of XOD has resulted into improved performance of xanthine biosensor with a detection limit 0.8 μM. The granular porous morphology of ZnO-NPs–PPy provides very sensitive and reliable biocompatible environment for the enzyme.

Appendix A. Supplementary data

Supplementary data associated with this article can be found, in the online version, at doi:10.1016/j.bios.2011.01.014.

References

Anik, U., Cubukcu, M., 2008. Turk. J. Chem. 32, 711–719.
Arslan, F., Yasar, A., Kilic, E., 2006. Art. Cells Blood Subst. Biotechnol. 34, 113–128.
Basu, A.K., Chattopadhya, P., RoyChoudhury, U., Chakraborty, R., 2005. Ind. J. Exp. Biol. 43, 646–653.
Berti, G., Fossati, P., Tarenghi, G., Musitelli, C., Melzid'Eril, G.V., 1988. J. Clin. Chem. Clin. Biochem. 26, 399–404.
Bose, C.S.C., Rajeshwar, K., 1992. J. Electroanal. Chem. 333, 235.
Chem, W., Li, C.M., Chen, P., Sun, C.Q., 2006. Electrochim. Acta 52, 1082.
Cioffi, N., Torsi, L., Sabbatini, L., Zambonin, P.G., Bleve-Zacheo, T., 2000. J. Electroanal. Chem. 488, 42.
Diaz, A.F., Kanazawa, K.K., Gardini, G.P., 1979. J. Chem. Soc. 1, 635.
Dimcheva, N., Horozova, E., Jordanova, Z., 2002. Anal. Chim. Acta. 57, 883.
Hu, S., Xu, C., Luo, J., Luo, J., Cui, D., 2000. Anal. Chim. Acta 412, 55–61.
Khan, R., Kaushik, A., Solanki, P.R., Ansari, A.A., Pandey, M.K., Malhotra, B.D., 2008. Anal. Chim. Acta 616, 207.
Kock, R., Delvoux, B., Gresiling, H., 1993. J. Clin. Chem. Clin. Biochem. 31, 303–310.
Kumar, S.A., Chen, S.M., 2008. Anal. Lett. 41, 141.
Li, Y.F., Liu, Z.M., Liu, Y.L., Yang, Y.H., Shen, G.L., Yu, R.Q., 2006. Anal. Biochem. 349, 33.
Li, X.H., Xie, Z.H., Min, H., Xian, Y.Z., Tongjin, L., 2008. Anal. Lett. 41, 456.
Liu, Y.C., Huang, J.M., Tsai, C.E., Chuang, T.C., Wang, C., 2004. Chem. Phys. Lett. 387, 155.
Liu, Y.C., Lee, H.T., Yan, S.J., 2006. Electrochim. Acta 51, 3441.
Lui, Y., Lo, N., Tao, W., Yao, S., 2004. Electroanalysis 16, 1271–1278.
Mao, L., Jin, L., Song, L., Yamamato, K., Jin, L., 1999. Electroanalysis 11, 499–504.
Mao, L., Xu, F., Xu, Q., Jin, L., 2001. Anal. Biochem. 292, 94–101.
Moghaddam, A.B., Nazari, T., 2008. Int. J. Electrochem. Sci. 3, 768.
Moghaddam, A.B., Badraghi, T.J., Kazemzad, M., 2009. Int. J. Electrochem. Sci. 4, 247–257.
Moody, G.J., Sanghera, G.S., Thomas, J.D.R., 1987. Analyst 112, 65–70.
Mulchandani, A., Luong, J.H.T., Male, K.B., 1989. Anal. Chim. Acta 221, 215–222.
Nabid, M.R., Golbabaee, M., Bayandori Moghaddam, A., Dinarvand, R., Sedghi, R., 2008. Int. Electrochem. Sci. 3, 1117.
Nakatani, H.S., Santos, L.V., Pelegrine, C.P., Gomes, M., Matsushita, M., Souza, N.E., Visentainer, J.V., 2005. Am. J. Biochem. Biotechnol. 1, 85–89.
Olojoa, R.O., Xiab, R.H., Abramsona, J.J., 2005. Anal. Biochem. 339, 338–344.
Pandey, P., Datta, M., Malhotra, B.D., 2008. Anal. Lett. 41, 157.
Pei, J., Li, X.Y., 2000. Anal. Chim. Acta 414, 205–213.
Phang, S.W., Tadokoro, M., Watanabe, J., Kuramoto, N., 2008. Curr. Appl. Phys. 8, 391.
Pundir, C.S., Devi, R., Narang, J., Singh, S., Shewta, J., 2011. J. Food Biochem (in press).
Rehak, M., Snejdarkova, M., Otto, M., 1994. Biosens. Bioelectron. 9, 337–341.
Renata, S., Pagliarussi, L., Luís, A.P., Freitas, L., Bastos, J.K., 2002. J. Sep. Sci. 25, 371–374.
Roux, S., De, G.L., Solerlllia, A.A., Champagne, S.D., Audebert, P., Sanchez, C., 2003. Adv. Mater. 15, 217.
Shah, L., 1996. J. Sci. Food Agric. 70, 298–302.
Shan, D., Wang, Y., Xue, H., Cosnier, S., 2009. Sens. Actuators B 136, 510–515.
Singh, S.P., Arya, S.K., Pandey, M.K., Malhotra, B.D., Saha, S., Sreenivas, K., Gupta, V., 2007. Appl. Phys. Lett. 91, 63901.
Wang, J.X., Sun, X.W., Wei, A., Lei, Y., Cai, X.P., Li, C.M., Dong, Z.L., 2006a. Appl. Phys. Lett. 88, 233106.
Wang, Z., Yang, Y., Li, Z., Gong, J., Shen, G., Yu, R., 2006b. Talanta 69, 686.
Westerfield, W.W., Richert, D.A., Higgins, E.S., 1959. J. Biol. Chem. 234, 1887.
Zhang, F., Wang, X., Ai, S., Sun, Z., Wan, Q., Zhub, Z., Xian, Y., Jin, L., Yamamoto, K., 2004. Anal. Chim. Acta 519, 155.
Zhao, G., Xu, J.J., Chen, H.Y., 2006. Anal. Biochem. 350, 145.
Zhou, H., Gan, X., Wang, J., Zhu, X., Li, G., 2005. Anal. Chem. 77, 6102.
Zhu, X., Yuri, I., Gan, X., Suzuki, I., Li, G., 2007. Biosens. Bioelectron. 22, 1600.